International Immunology, Vol. 17, No. 2, pp. 177–191
doi:10.1093/intimm/dxh198 Advance Access publication 3 January 2005

Over-expressed IgG2 antibodies against *O*-acetylated sialoglycoconjugates incapable of proper effector functioning in childhood acute lymphoblastic leukemia

Suman Bandyopadhyay[1], Arindam Bhattacharyya[2], Asish Mallick[1], Asish Kumar Sen[3], Gayatri Tripathi[4], Tanya Das[2], Gaurisankar Sa[2], Dilip Kumar Bhattacharya[5] and **Chitra Mandal[1]**

[1]Immunobiology Division, Indian Institute of Chemical Biology, 4 Raja S.C. Mullick Road, Jadavpur, Kolkata 700 032, India
[2]Bose Institute, P-1/12 CIT Scheme VII M, Kolkata 700 054, India
[3]Department of Organic Chemistry and [4]Cell Physiology Division, Indian Institute of Chemical Biology, 4 Raja S.C. Mullick Road, Jadavpur, Kolkata 700 032, India
[5]Department of Pathology, Vivekananda Institute of Medical Sciences, 99 Sarat Bose Road, Kolkata 700 019, India

Keywords: anti-9-*O*AcSGs, effector function, glycosylation, subclass

Abstract

Earlier studies have demonstrated an over-expression of 9-*O*-acetylated sialoglycoconjugates (9-*O*AcSGs) on lymphoblasts, concomitant with high titers of anti-9-*O*AcSGs in childhood acute lymphoblastic leukemia (ALL). The present study was aimed to evaluate whether this high induction of anti-9-*O*AcSGs at disease presentation contributes toward immune surveillance. Accordingly, anti-9-*O*AcSGs were affinity purified from sera of ALL patients and normal individuals, and their specificity toward the glycotope having terminal 9-*O*-acetylated sialic acid-linked subterminal *N*-acetyl galactosamine (GalNAc) in α2–6 manner (9-*O*AcSAα2–6GalNAc) was established by hemagglutination assay, flow cytometry and confocal microscopy. Subclass distribution of anti-9-*O*AcSGs revealed a predominance of IgG2 in ALL. Analysis of glycosylation of anti-9-*O*AcSGs purified from sera of ALL patients (IgG_{ALL}) and normal individuals (IgG_N) by digoxigenin glycan enzyme assay, fluorimetric estimation, gas–liquid chromatography and lectin-binding assays demonstrated that disease-specific antibodies differ in content and nature as compared with normal controls. Enhanced amount of 9-*O*AcSA-specific IgG2 induced in ALL was unable to trigger activation of FcγR, the complement cascade and cell-mediated cytotoxicity, although its glycotope-binding ability remains unaffected. Interestingly, only $IgG1_N$ emerged as the potent mediator of cell-mediated cytotoxicity, complement fixation and activator of effector cells through FcγR. In ALL, the observed subclass switching of anti-9-*O*AcSGs to IgG2, alteration in their glycosylation profile along with impairment of a few Fc-glycosylation-sensitive effector functions hints toward a disbalanced homeostasis, thereby evading the host defense. These findings justify further evaluation of the mechanism for functional unresponsiveness of antibodies and production of 9-*O*AcSA-specific chimeric antibodies with normal Fc domain for therapeutic applications.

Introduction

Acute lymphoblastic leukemia (ALL) is a malignant transformation of lymphoblasts and represents the single most common type of cancer in the pediatric population (1). The cure rates have increased to 80% due to improved diagnostics, identification of risk factors and intensification of risk-directed therapy. Although current treatment protocols induce complete remission in >80% of children, a 20% risk of relapse remains as patients in remission may harbor minimal residual disease, not identifiable by routine cytomorphology (2).

Sialic acids (originally abbreviated as Neu5Ac), a family of acidic nine-carbon sugars, are typically located at the terminal positions of glycoconjugates of cell membranes and play

Correspondence to: C. Mandal; E-mail: cmandal@iicb.res.in

Transmitting editor: A. Falus

Received 19 May 2004, *accepted* 17 November 2004

a significant role in the mediation of many biological phenomena involving cell–cell interactions either by reacting with specific surface receptors or via masking of carbohydrate recognition sites (3, 4). Among the diverse multitude of variations of Neu5Ac, the most frequently occurring modification is *O*-acetylation at positions C-7, -8 and -9 to form *N*-acetyl-7, -8, -9-*O*-acetyl neuraminic acid, respectively, thus generating a family of *O*-acetylated sialoglycoconjugates (*O*-AcSGs) (5). However, as *O*-acetyl esters from C-7 and C-8 positions spontaneously migrate to C-9 position, even under physiological conditions, the *O*-acetylation at C-9 position [9-*O*-acetylated sialic acid (9-*O*AcSA)] is considered as the commonest biologically occurring modification (6, 7).

The binding specificity of Achatinin-H, a 9-*O*AcSAα2–6GalNAc-binding lectin, purified from the hemolymph of the African giant land snail, *Achatina fulica* (8–11), allowed us to identify an enhanced expression of five molecules having terminal 9-*O*AcSA corresponding to 36, 90, 120, 135 and 144 kDa on PBMC of ALL patients; a basal level of expression of only two molecules having terminal 9-*O*AcSA (36 and 144 kDa) was identified on PBMC from normal individuals (3, 7, 12, 13). An increased antibody (anti-9-*O*AcSGs) production against these glycoproteins in these children confirmed its immunogenicity (14–16). Importantly, no cross-reactivity was observed with patients having other hematological disorders (3, 12–16). At disease presentation, high titers of immune-complexed 9-*O*AcSGs were observed in these patients' sera (17). These circulating anti-9-*O*AcSGs (free as well as immune complexed) have been successfully utilized for diagnosis and monitoring of the disease status (13–17).

A central question in cancer immunology is whether recognition of tumor antigens by the immune system initiates activation (i.e. surveillance) or functional unresponsiveness. Paradoxically, while strong evidence exists that specific immune-surveillance systems operate at early stages of tumorigenesis, immune unresponsiveness is a feature of established tumors (18). It is now recognized that tumors can directly or indirectly impede the development of anti-tumor immune responses through immunosuppressive cytokines (transforming growth factor-β and IL-10), T cells with immunosuppressive activities (regulatory T cells, 19), inactivation of death receptor signaling pathways (20) or expression of anti-apoptotic signals (21). Tumor escape can also result from changes that occur directly in the tumor, such as loss of antigen expression, loss of MHC components (22) and development of IFNγ insensitivity (23). This induction of unresponsiveness by tumors can occur either through anergy or through deletion from resistance mechanisms to recognition and killing of tumor cells by activated immunological effectors. In pediatric ALL, the role of antibodies induced against disease-associated glycotopes remains obscure and accordingly, this study aims to explore their role in immune surveillance to understand the disease biology.

The present study has focused on (i) affinity purification of anti-9-*O*AcSGs, (ii) analysis of their subclass distribution, (iii) determination of their total glycosylation and sialylation profile and (iv) evaluation of the functional activity exerted by anti-9-*O*AcSGs.

Methods

Patients and controls

This study included sera from children with confirmed ALL (n = 50), at presentation of disease, admitted at Vivekananda Institute of Medical Sciences, Kolkata. Clinical information and blood samples were sent to Indian Institute of Chemical Biology. The diagnosis of leukemia was made by standard cytomorphological and histochemical examination of bone marrow and blood smears according to French–American–British classification (24) and by immunophenotyping using a panel of mAb that included CD 2, 3, 7, 10, 19, 20, 36, 45, 13, 33 and 34 and HLA-DR. The diagnosis was further validated by FACS analysis using an in-house probe, Achatinin-H (12, 13), specific for 9-*O*AcSAα2–6GalNAc glycotopes. Patients with L3 morphology (according to French–American–British criteria) were excluded. The male/female ratio was 2 : 1, and median age was 6.2 years with a range of 1.1–17.3 years. Controls were age-matched normal healthy donors (n = 20). Informed consent was taken from parents and patients. The Institutional Human Ethical Clearance Committee approved the study.

Cell lines

The REH (human B-ALL) and U937 (human promonocytic) cell lines were purchased from American Type Culture Collection (Manassas, VA, USA). The CEM-C7, a human T-ALL cell line, was a kind gift from Reinherd Schwartz-Albiez, Deutsches Krebsforschungszentrum, Heidelberg, Germany (13). The cells were cultured in RPMI-1640 medium supplemented with 10% (v/v) heat-inactivated FCS, 0.002 M L-glutamine, antibiotics and antimycotics (medium A).

Chemicals and reagents

All chemicals unless stated otherwise were purchased from Sigma, St. Louis, MO, USA.

Probes

Preparation of bovine submaxillary mucin and its derivatives. Bovine submaxillary glands were used for purification of bovine submaxillary mucin (BSM) (25), and protein content was measured (26). The percentage of 9-*O*AcSA was demonstrated by fluorimetric HPLC (27) and quantified as 22.5% by fluorimetric estimation (28).

BSM was de-sialylated (asialo BSM) and de-*O*-acetylated (de-*O*Ac BSM) by incubating with 0.25% H_2SO_4 (0.045 M) for 1 h at 80°C and by alkaline hydrolysis with NaOH (0.01 M) for 1 h at 4°C, respectively.

Purification of Achatinin-H. Following activation of Sepharose 4B (Amersham Biosciences, Uppsala, Sweden) (29), activated beads were coupled separately with BSM and asialo BSM (5 mg ml^{-1} gel). Achatinin-H was affinity purified from the hemolymph of *A. fulica* snails using BSM–Sepharose 4B (8) as it contains a high proportion of 9-*O*AcSAs linked with subterminal *N*-acetyl galactosamine (GalNAc) of the underlying oligosaccharide chain (30). Carbohydrate-binding specificity of purified Achatinin-H toward 9-*O*AcSAα2–6GalNAc was established (8) and used as a probe in FACS analysis and for affinity purification of 9-*O*AcSGs.

Purification and characterization of anti-9-OAcSGs. Pooled sera (~10 ml) from ALL patients at presentation of the disease, i.e. before any treatment and normal controls, were used to purify anti-9–*O*AcSG fractions with preferential affinity for 9-*O*AcSAα2–6GalNAc using the method of Pal *et al.* (15). Briefly, serum was subjected to a 33% ammonium sulfate fractionation and sequentially passed through asialo BSM–Sepharose, BSM–Sepharose and Protein A–Sepharose column (Amersham Biosciences, Uppsala, Sweden). Different subclasses of IgG were eluted with sodium citrate (0.1 M) using a pH gradient that ranged from pH 6.0–1.0 followed by immediate neutralization with 2.0 M Tris and extensive dialysis against PBS. Purity was tested by SDSP (10%, 31) and subsequent western blotting using HRP-conjugated goat anti-human IgG (Jackson ImmunoReasearch Laboratories, Inc., West Grove, PA, USA). The specificity of Ig subclasses of all these purified fractions was confirmed by an ELISA.

Specificity of purified anti-9-OAcSGs toward 9-OAcSAα2–6GalNAc

Hemagglutination activity. The biological activities of the purified antibody fractions were checked by hemagglutination (HA) (8). The HA titer was reported as the reciprocal of the highest antibody dilution giving complete agglutination.

The sugar specificity of purified anti-9-*O*AcSGs was confirmed using different sugars (8), and the concentration of sugar needed for 100% inhibition of HA was determined using a fixed concentration (16 HA units) of purified antibody.

Flow cytometric analysis revealed binding of purified antibodies to 9-OAcSGs on PBMC of ALL patients. Purified anti-9-*O*AcSGs were conjugated with FITC (32). The binding of FITC–anti-9-*O*AcSGs (0.5 μg per 10^6 cells) to cell lines, B-(REH) and T-ALL (CEM-C7, MOLT-4) and PBMC from both B-(n = 22) and T-ALL (n = 6) patients along with PE-conjugated anti-CD 19 or anti-CD 7 (known as B- and T-cell marker, respectively, BD, Palo Alto, CA, USA) was examined by staining with respective probes for 1 h at 4°C in the dark (33). The binding was assessed using a FACSCalibur flow cytometer (BD, Palo Alto, CA, USA) and analyzed by CELLQUEST software (BD, Palo Alto, CA, USA). To confirm the epitope specificity of purified Igs, cells were pre-incubated with cold Achatinin-H or pre-treated with *O*-acetyl esterase, an enzyme capable of cleaving the 9-*O*-acetyl group from Neu5Ac (27), and binding of FITC–anti-9-*O*AcSGs was determined. Isotype-matched antibodies served as controls. For each analysis, 10 000 events were recorded.

Confocal microscopy demonstrated binding of purified anti-9-OAcSGs to ALL cell surface. To visualize the binding of purified anti-9-*O*AcSGs to PBMC from both B- and T-ALL patients and T- and B-ALL cell lines (CEM-C7, MOLT-4 and REH), cells were incubated with FITC-antibodies and observed under a confocal microscope. Briefly, cells (1×10^5 cells per 50 μl) were adhered on poly-L-lysine-coated glass cover slips for 1 h at 20–25°C, fixed with PFA (1%, 100 μl) for 30 min on ice followed by incubation with ammonium chloride (50 mM, 100 μl) for 5 min on ice. After washing with PBS, they were incubated with FITC–anti-9-*O*AcSGs (0.005 μg) for 20 min on ice in the dark. After washing and mounting, cells were examined under a confocal scanning microscope (Leica SP2, Leica, Wetzlar, Germany); the slides were illuminated with a 488-nm laser, and images were collected using a band-pass filter (505–550 nm) with the pinhole set at 100 μm.

Quantification of circulating anti-9-OAcSGs. Microtiter plates were coated with purified BSM (1.0 μg per 100 μl per well) in 0.02 M phosphate buffer, pH 7.4, overnight at 4°C. Sera (1 : 10 dilution) were added to the BSM-coated wells, whose non-specific binding sites had been previously blocked with PBS containing 2% BSA, and incubated overnight at 4°C. The plates were washed and incubated with different subclasses of murine anti-human IgG (diluted 1 : 3000, 100 μl per well, Dianova, Hamburg, Germany), and specific bindings were captured using HRP-conjugated anti-murine IgG (diluted 1 : 10 000, 100 μl per well, (Jackson ImmunoReasearch Laboratories, Inc., West Grove, PA, USA) and detected at 405 nm in a Multiskan MS Lab Systems ELISA reader using azino-bis thio-sulfonic acid (Roche Molecular Biochemicals, Mannheim, Germany) as the substrate. Standard curves generated using increasing amounts of affinity-purified anti-9-OAcSGs (0–20 μg per 100 μl per well) were applied for quantitation of anti-9-*O*AcSGs present in sera.

Analysis of glycosylation of affinity-purified anti-9-OAcSGs

Detection of total glycosylation and sialylation by digoxigenin enzyme assay. The degree of glycosylation and sialylation was evaluated by placing an equal amount (1.0 μg per 5.0 μl) of IgG_{ALL} and IgG_N by a digoxigenin (DIG) enzyme assay using a DIG glycan detection kit (Roche Molecular Biochemicals, Mannheim, Germany) according to manufacturer's instructions. DIG-labeled glycoconjugates, present on nitrocellulose paper, were detected using alkaline phosphatase-conjugated anti-DIG antibody and visualized with 4-nitroblue tetrazolium chloride/5-bromo-4-chloro-3-indolyl phosphate as substrate. The developed spots were scanned and quantified in arbitrary units using Image Master Totallab Software, version 1.11 (Amersham Pharmacia Biotech, Sweden). Equal amounts (5.0 μg per 5.0 μl) of transferrin and creatinase were used as positive and negative controls, respectively.

Quantitation of total Neu5Ac and 9-OAcSA by fluorimetric estimation. Quantitation of total Neu5Ac and 9-*O*AcSA was performed fluorimetrically (28) by oxidizing purified antibodies (3.0 μg) and processed using acetyl acetone method with or without saponification of the *O*-acetyl groups of Neu5Acs. The relative fluorescence intensity [$\lambda_{max(excitation=410nm)}/\lambda_{max(emission=510nm)}$] of each sample was measured against reagent blanks on a Hitachi F-4010 spectrofluorimeter (Tokyo, Japan). The Neu5Ac content was determined from standard curves obtained using pure Neu5Ac. The values obtained for the de-*O*-acetylated samples indicated total Neu5Ac content, while the percentage of (8)9-*O*-acetylated Neu5Ac was determined by subtracting the respective unsubstituted Neu5Acs from that obtained after de-*O*-acetylation.

Detection of neutral sugars by gas–liquid chromatography. Neutral sugars present in the anti-9-*O*AcSGs were detected by gas–liquid chromatography (GLC) as their alditol acetates (34). The 9-*O*AcSA-specific IgGs (100 μg each) were hydrolyzed with trifluoroacetic acid (2.0 M) at 120°C for 90 min, followed by reduction with sodium borohydride (10 mg). Resulting alditols were acetylated with acetic anhydride in distilled pyridine [1 ml, 1 : 1 (v/v)] at 22–25°C for 16 h and analyzed by GLC using a Hewlett-Packard 6890 plus

gas chromatograph equipped with a flame ionization detector. The constituent sugars were identified from the retention time of authentic sugars. For the detection and quantification of the peaks, a Hewlett-Packard 3380A chemstation was used. For resolution, a fused-silica capillary column HP-5 (30 m, 0.32 mm, 0.25 μm) and nitrogen as carrier gas were used with a temperature program of 150°C (5 min), 2°C (1 min) and 200°C (10 min) at splitless mode.

Detection of terminal sugar by DIG glycan differentiation kit. The presence of terminal sugars along with their specific linkages was analyzed by DIG glycan differentiation kit (Roche Molecular Biochemicals, Mannheim, Germany) using several plant lectins, namely *Galanthus nivalis* agglutinin (GNA), *Sambucus nigra* agglutinin (SNA), *Maackia amurensis* agglutinin (MAA), peanut agglutinin (PNA) and *Datura stramonium* agglutinin (DSA), as per the manufacturer's protocol.

Lectin bead-binding assay. The purified 9-*O*AcSA-specific IgG1 and IgG2 from ALL patients and normal individuals were iodinated with ^{125}I-Na using the chloramine T method (35). Fixed concentrations (0.2 μg) of ^{125}I-IgG1 and/or IgG2 were incubated separately with Sepharose/agarose-bound lectins (20 μl) of different linkage and specificity, e.g. Con A, *Ricinus communis* agglutinin (RCA), *Dolichos biflorus* agglutinin (DBA), *Helix pomatia* agglutinin (HPA), wheat germ agglutinin (WGA), *Ulex europaeus* agglutinin (UEA), *Limulus polyphemus* agglutinin (LPA), MAA, SNA, and Achatinin-H, overnight at 4°C. The beads were initially incubated with 2% BSA in PBS or Tris-buffered saline (TBS) to block non-specific binding sites. Following removal of unbound antibody fractions, specifically bound antibodies were monitored in a gamma counter. Unconjugated Sepharose/agarose beads served as controls. Binding (%) was calculated as follows:

$$\text{Binding}\,(\%) = \frac{\text{bound count} - \text{control count}}{\text{Total counts of } ^{125}\text{I-antibody used for a particular set}} \times 100.$$

All experiments were performed twice in triplicate.

Evaluation of generation of intracellular reactive oxygen species as an index for effector cell activation through FcγR. Intracellular reactive oxygen species (ROS) generation was monitored using a cell-permeable probe 2′,7′-dichlorofluorescein diacetate (H_2DCFDA, Molecular Probes, Eugene, OR, USA), which is oxidized to a fluorescent compound 2′,7′-dichlorofluorescein in the presence of an oxidant.

U937 cells were used to analyze the interaction between FcγR present on its surface and the Fc region of anti-9-*O*AcSGs, resulting in the triggering of a respiratory burst that is considered as an indicator of cell activation. The cells were cultured in medium A in the presence of IFNγ (1000 U ml^{-1}) for 2 days to induce differentiation and the capacity to generate superoxide.

To pinpoint the binding of the Fc region of anti-9-*O*AcSGs with FcγR present on U937 cells, Fab paratopes of these antibodies (total IgG, IgG1and IgG2) were blocked by incubating them with BSM (1 mg ml^{-1}) and/or purified 9-*O*AcSGs (0.03 mg ml^{-1}) at 4°C for 1 h.

These Fab-blocked anti-9-*O*AcSGs (0.5 μg) were allowed to bind with IFNγ-sensitized U937 cells (1×10^6 cells) for 1 h at 37°C and incubated with H_2DCFDA (2 μg ml^{-1}) for 30 min at 37°C in the dark. Following washing, they were analyzed by flow cytometry and also visualized under a confocal microscope as described earlier. In confocal microscopy, slides were analyzed in triplicate and total fluorescence was expressed as fluorescence intensity units (FIU) at 530 nm. Cells incubated only with BSM and/or purified 9-*O*AcSGs in the absence of antibodies served as controls.

Activation of the classical complement pathway. Purified anti-human C3α chain mAb, SIM 27-49 (36), was iodinated with ^{125}I-Na (35) and used for measuring C3 deposition on the cell surface due to activation of the classical complement pathway triggered by anti-9-*O*AcSGs. Sera (20%) from normal individuals and/or untreated ALL patients were used as the source of the complement.

Cells (CEM-C7 and REH, 2×10^6 per 100 μl) were suspended in TBS and allowed to bind with purified anti-9-*O*AcSGs (0.1-1.0 μg) as complement activators at 37°C for 30 min. EDTA (10 mM) was always used as the blocker of alternative pathway of complement activation. Following washing, the cells were incubated with complement (100 μl) for 10 min at 37°C and washed twice in cold TBS, and the amount of C3 deposition on the cell surface was quantitated by incubating further with ^{125}I-anti-C3 mAb (2×10^5 counts per minute) for 1 h on ice. After two washes, the radioactivity incorporated in C3–anti-C3 complexes was determined by a gamma counter. Each set was repeated thrice. Cells incubated with complements or complement activators alone or complement activators in the presence of heat-inactivated complement served as different controls.

Evaluation of cytotoxic potential of anti-9-OAcSGs by ^{51}Cr-release antibody-dependent cell-mediated cytotoxicity assay. ALL cell lines (CEM-C7 and REH) were suspended in medium A with human AB serum (10%) and labeled with $Na_2{}^{51}CrO_4$ (0.1 mCi per 1×10^6 cells, BARC, Mumbai, India; 37) in the presence and absence of purified anti-9-*O*AcSGs$_{ALL}$ and anti-9-*O*AcSGs$_N$ (IgG1 and IgG2, 1.0 μg) for 3 h at 37°C and 5% CO_2. Cells were washed with the same medium and used as target cells. Freshly isolated normal human PBMC were used as effector cells. Target (1×10^4 cells per 100 μl per well) and effector cells were co-incubated in a 96-well U-bottom tissue culture plate for 16 h at 37°C in a 5% CO_2 environment at E : T ratios of 5 : 1, 25 : 1, 50 : 1 and 100 : 1. The plate was centrifuged at 500 × *g* for 5 min, and the supernatants were checked for released ^{51}Cr by a gamma counter. Spontaneous release and maximum release (100% lyses) of ^{51}Cr from labeled target cells were evaluated in the absence of effector cells and on treatment with 5% (v/v) Triton X-100, respectively. Cytotoxicity was calculated as: 100 × [(experimental counts − spontaneous counts)/(maximum counts − spontaneous counts)]. Specific cell lyses (%) were calculated by normalizing the background cytotoxicity in the absence of added antibody. All assays were done in triplicate wells and three independent experiments were performed for each set.

Interaction of antibodies with Staphylococcal protein A and Streptococcal protein G. ^{125}I-Labeled anti-9-*O*AcSGs (IgG1 and IgG2, 0. 2 μg) purified from ALL and normal sera were separately incubated with Sepharose–Staphylococcal protein A (SpA) and Streptococcal protein G (SpG) (20 μl) overnight at 4°C and specific counts were analyzed as described earlier.

Experiments were performed in triplicate, and unconjugated beads served as controls.

Statistical analysis

Results are reported as mean ± SD. Statistical analyses were performed using the Graph-Pad Prism statistics software (Graph-Pad Software Inc., San Diego, CA, USA). Student's unpaired *t*-tests were used. Reported values are two tailed and *P* values <0.05 were considered as statistically significant at 95% confidence interval.

Results

Anti-9-OAcSGs predominantly belong to IgG2 subclass in ALL

Analysis of sera for subclass distribution of anti-9-*O*AcSGs demonstrated a 2.78-fold higher concentration of $IgG2_{ALL}$ as compared with $IgG1_{ALL}$ (158.1 ± 5.57 versus 56.67 ± 3.63 μg ml^{-1}, respectively, $P < 0.0001$) and a 3-fold increase in $IgG2_{ALL}$ was quantified than $IgG2_N$ (158.1 ± 5.57 versus 51.26 ± 4.80 μg ml^{-1}, respectively, $P < 0.0001$). However, the patient/normal ratio for IgG1, IgG3 and IgG4 subclasses was lower, being 1.83 ($P < 0.0001$), 2.29 ($P < 0.0001$) and 1.34 ($P < 0.01$), respectively (Fig. 1). The levels of 9-*O*AcSA-specific $IgG3_{ALL}$ and $IgG4_{ALL}$ were very low, being 21.26 ± 1.12 μg ml^{-1} and 18.86 ± 1.84 μg ml^{-1}, respectively.

Purified anti-9-OAcSGs are specific for the glycotope Neu5,9Ac$_2$α2–6β-D-GalNAc

Purification of anti-9-*O*AcSGs revealed a 3-fold higher induction of IgG_{ALL} as compared with IgG_N (96.29 ± 4.22 versus 31.46 ± 3.07 μg ml^{-1}, respectively). The specificity of purified anti-9-*O*AcSGs was analyzed by a HA assay. Rabbit erythrocytes, containing a high percentage of 9-*O*AcSA on their cell surface, showed a maximum HA titer, whereas human erythrocytes of different blood groups, which contain only Neu5Ac and importantly no 9-*O*AcSA (38), did not agglutinate (Table 1). Although the percentage of 9-*O*AcSA in the other species had a narrow range of 20–25%, a far wider variation in the HA titer was observed, possibly reflecting the variability in accessibility of the 9-*O*AcSA residues. The specificity of these antibody fractions toward Neu5,9Ac$_2$α2–6β-D-GalNAc was further substantiated by HA inhibition assays using free 9-*O*AcSA as well as several sialoglycoproteins (Table 2). All four subclasses of antibodies preferentially bound to BSM having terminal 9-*O*AcSA and subterminal GalNAc in an α2–6 linkage. The absence of inhibition with de-*O*Ac BSM, asialo BSM, SSM, HCG and fetuin reconfirmed its specificity. However, the antigens present in BSM could be either in a mono-, di-, or tri-*O*-acetylated form, which the purified antibody possibly cannot distinguish.

Purified anti-9-OAcSGs bind to ALL blasts but not with normal PBMCs

Flow cytometric analysis revealed that FITC–anti-9-*O*AcSGs$_{ALL}$ bind strongly with $PBMC_{ALL}$ (87–99%, $n = 28$) irrespective of their lineage, whereas $PBMC_N$ showed negligible binding (8–14%, $n = 14$). This binding was confined to *O*-AcSGs as the antibody binding was reduced in $PBMC_{ALL}$ by 87.5% when cells were pre-incubated with 5.0 μg unconjugated Achatinin-H prior to incubation with FITC–anti-9-*O*AcSGs$_{ALL}$ (96 versus 12%, Fig. 2A). Similarly, their pre-treatment with *O*-acetyl esterase caused 85–92% reduction. ALL cell lines (both B and T) also showed similar binding profiles.

These purified antibodies consistently demonstrated surface binding with $PBMC_{ALL}$ and cell lines, irrespective of the lineages, as evidenced by confocal microscopy (Fig. 2B); binding with normal PBMCs was negligible (data not shown).

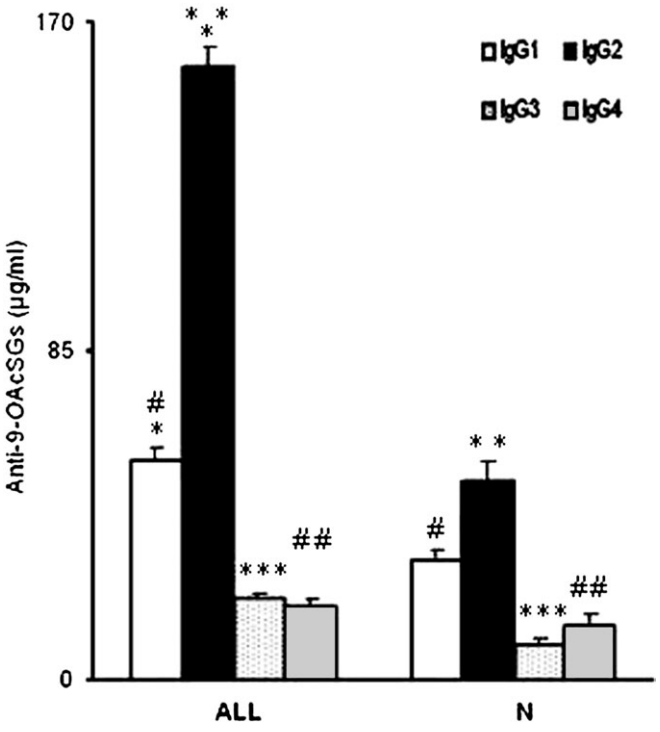

Fig. 1. Subclass distribution of 9-*O*AcSA-specific IgGs in ALL patients and normal individuals. Levels of anti-9-*O*AcSGs: IgG1 (open bar), IgG2 (filled bar), IgG3 (dotted bar) and IgG4 (shaded bar) were quantified in sera of ALL patients at disease presentation along with normal donors (N) by an ELISA using BSM as coating antigen as described in Methods. Data are expressed as mean ± SD of absolute quantitation (μg ml^{-1}). Significant differences between mean values: $*P < 0.0001$; $**P < 0.0001$; $***P < 0.0001$; $\#P < 0.0001$ and $\#\#P < 0.01$.

Table 1. HA of erythrocytes by purified anti-9-*O*AcSGs

Erythrocytes[a]	Position of major *O*-acetylated group	*O*AcSA content (%)[b]	HA[c]
Human A	—	0	0
Human B	—	0	0
Human O	—	0	0
Guinea pig	C-9	22	8
Rabbit	C-9	20	512
Rat	C-9	25	4
Hamster	C-9	22	8

[a]Erythrocytes (2%, v/v) were incubated with purified antibody fractions for their agglutination (8). [b]Fluorimetric estimation of percentage of 9-*O*-acetylated Neu5Acs according to the method of Shukla and Schauer (28). [c]The HA titer was reported as the reciprocal of the highest antibody dilution giving complete agglutination. Four subclasses of anti-9-*O*AcSGs showed comparable results.

Anti-9-OAcSGs in ALL patients (IgG_{ALL}) differ in the nature and content of glycosylation from those of normal individuals (IgG_N)

The degree of glycosylation (Fig. 3A and B) and specifically sialylation (Fig. 3C) of 9-*O*AcSA-specific purified IgGs was demonstrated using the DIG glycan detection kit. A 2.1-fold increase in overall glycosylation was observed in IgG_{ALL} as compared with IgG_N, the mean ± SD of densitometric score in arbitrary units being 80 651 ± 8210 versus 38 232 ± 5100, respectively, $P < 0.0006$ (Fig. 3B).

However, the Neu5Ac content was 3.6-fold higher in ALL patients than normal controls (densitometric scores being 15 207 ± 2370 versus 4224 ± 642, respectively, $P < 0.008$, Fig. 3C). The presence of high amount of Neu5Acs in anti-9-*O*AcSGs$_{ALL}$ was corroborated by fluorimetric estimation of their (IgG, IgG1 and IgG2) Neu5Ac content as compared with their normal counterparts, the concentrations being 3.3- ($P < 0.0002$), 2.9- ($P < 0.0001$) and 3.2-fold ($P < 0.005$) higher in ALL antibodies, respectively. Interestingly, Neu5Ac content of $IgG2_{ALL}$ was found to be higher than $IgG1_{ALL}$, mean ± SD being 40.0 ± 2.0 versus 25.3 ± 1.6 ng of Neu5Ac per 1.0 μg of Igs ($P < 0.0006$, Fig. 3D). However, no measurable difference was observed in the (8)9-*O*-acetylated Neu5Ac content of antibody fractions in ALL patients versus normal controls.

To trace the content of individual neutral sugars present in anti-9-*O*AcSGs purified from ALL patients and normal individuals, GLC analysis was performed. The gas–liquid chromatogram peaks revealed a significantly higher amount of *N*-acetyl glucosamine (GlcNAc) in IgG_{ALL} (Fig. 4A) and galactose (Gal) in IgG_N (Fig. 4B). As compared with normal controls, IgG_{ALL}

Table 2. Sugar specificity of purified anti-9-*O*AcSGs by HA inhibition assays

Sugars	Terminal linkages	Relative inhibitory potency (%)[a]
Monosaccharide	$Neu5,9Ac_2$	0.17
BSM	$Neu5,9Ac_2$α2–6β-D-GalNAc	100.00
de-*O*Ac BSM	Neu5Acα2–6β-D-GalNAc	Nil
Asialo BSM	GalNAc	Nil
SSM	Neu5Acα2–6β-D-GalNAc	Nil
HCG	Neu5Acα2–3β-D-Gal	Nil
Fetuin	Neu5Acα2–6β-D-Gal	Nil

SSM, sheep submaxillary mucin; HCG, human chorionic gonadotrophin; and Nil, no inhibition. Four subclasses of anti-9-*O*AcSGs showed comparable result.

[a]The minimal concentration of sugars or glycoproteins required for total inhibition of HA of rabbit erythrocytes (2%, v/v) induced by 16 HA units of purified anti-9-*O*AcSGs is the inhibitory concentration/potency (8). Considering the inhibitory potency of BSM as 100, the relative inhibitory potency of different sialoglycoproteins/sugars are calculated.

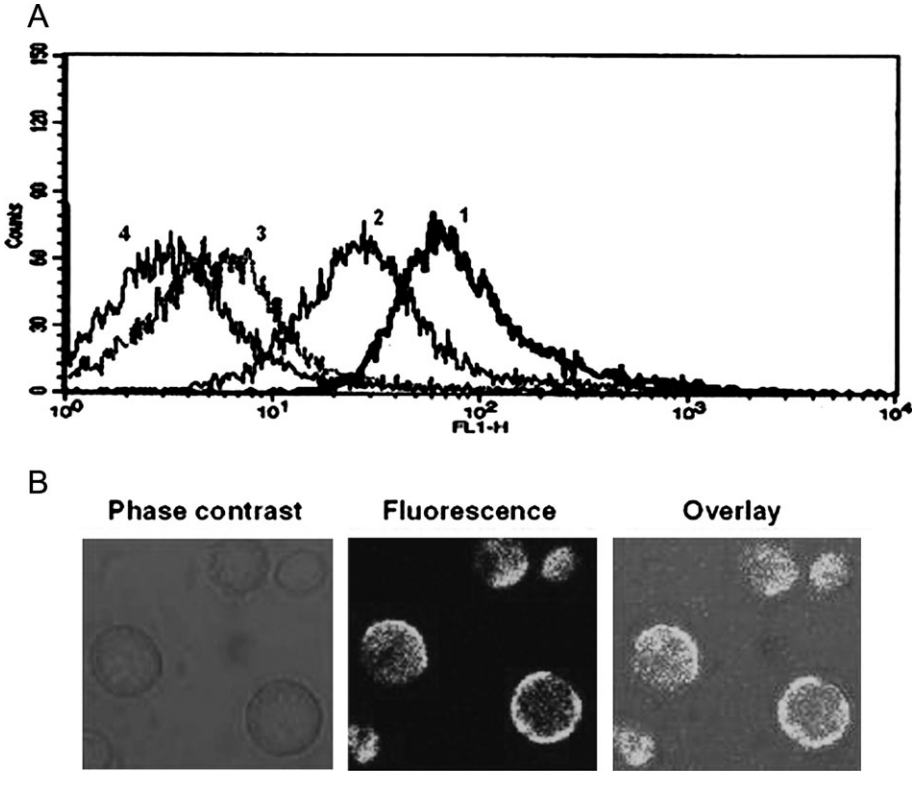

Fig. 2. (A) Purified anti-9-*O*AcSGs bind to lymphoblasts of ALL patients. A representative profile of the flow cytometric analysis revealing specific binding of affinity-purified FITC–anti-9-*O*AcSGs to $PBMC_{ALL}$ as described in Methods. Peaks 1 and 2 represent high expression of 9-*O*AcSGs on $PBMC_{ALL}$ using FITC–anti-9-*O*AcSGs ($IgG1_{ALL}$) and FITC–Achatinin-H, respectively. Specificity of antibody binding was demonstrated by binding of anti-9-*O*AcSGs to $PBMC_{ALL}$ following pre-incubation with unconjugated Achatinin-H (peak 3). Peak 4 represents binding with control antibody. (B) Visualization of binding of anti-9-*O*AcSGs to the ALL cell surface by confocal microscopy. FITC–anti-9-*O*AcSGs were targeted toward $PBMC_{ALL}$ (1×10^5 cells per 50 μl) of both the lineages, ALL cell lines as well as $PBMC_N$, for 20 min on ice in the dark and visualized under a confocal scanning microscope (Leica SP2, Leica, Wetzlar, Germany) as described in Methods. A representative slide consisting of phase contrast, fluorescence and overlaid images of ALL PBMC is documented.

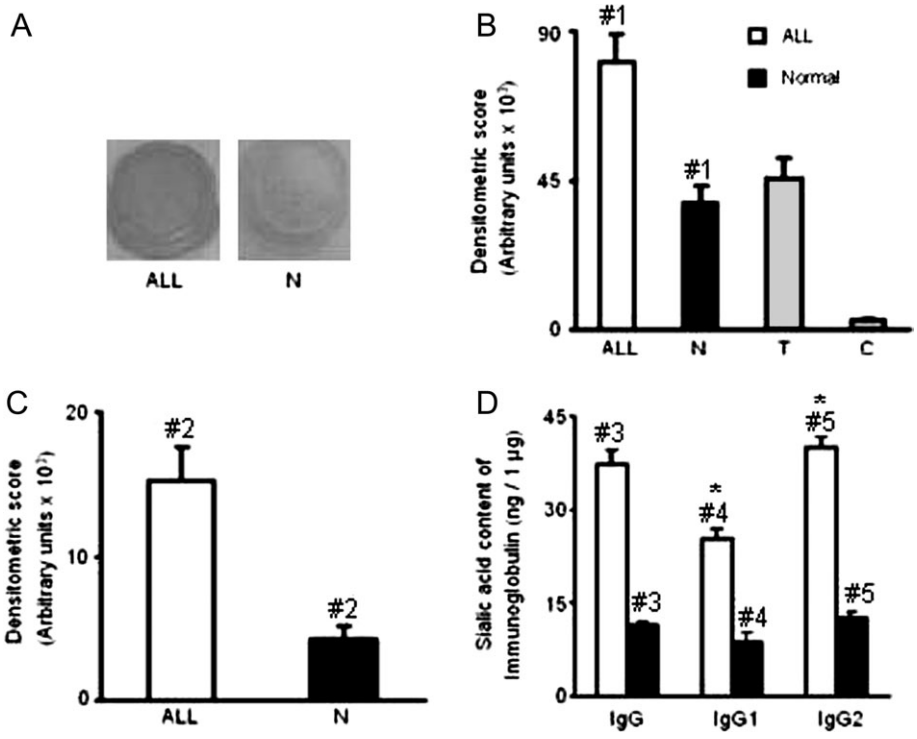

Fig. 3. Differential glycosylation and sialylation of anti-9-*O*AcSGs. (A) A representative profile of glycosylation pattern in anti-9-*O*AcSGs (IgG) of ALL patients ($n = 4$, ALL) and normal donors ($n = 4$, N). Equal amounts (1.0 µg) of affinity-purified Igs were blotted on to nitrocellulose membrane and processed for the detection of neutral sugars using a DIG glycan detection kit. (B) The intensities of the developed spots were quantified using Image Master Totallab Software, version 1.11 (Amersham Pharmacia Biotech). Results were reported as mean ± SD of densitometric score in arbitrary units from two independent experiments. Transferrin (T) and creatinase (C) were used as positive and negative controls, respectively. #1, significant differences between mean values, $P < 0.0006$. (C) The degree of sialylation of all these samples were detected by DIG enzyme assay using DIG glycan detection kit as described in Methods. Spot intensities were stated as mean ± SD of densitometric score in arbitrary units. #2, significant differences between mean values, $P < 0.008$. (D) The Neu5Ac contents in purified anti-9-*O*AcSGs were detected by fluorimetric estimation. Purified antibodies from ALL patients (open bar) and normal individuals (filled bar) were processed as described in Methods (27). Significant differences between mean values, #3, $P < 0.0002$; #4, $P < 0.0001$; #5, $P < 0.005$ and *, $P < 0.0006$.

had a higher amount of GlcNAc (relative percent area of the peak being 6.86 versus 29.88), GalNAc (4.81 versus 9.04%) and mannose (10.24 versus 13.28%), whereas the amount of Gal was marginally higher in IgG_N than IgG_{ALL} (32.002 versus 21.64%, respectively, Fig. 4A and B).

Although GLC analysis showed differences in the total content of neutral sugars, it would be interesting to explore the linkage-specific arrangement of terminal sugars of IgG-glycans. With this view, we have exploited the binding specificity of various well-established lectins toward known terminal sugar moiety in the analysis of glycans present in anti-9-*O*AcSGs (IgG1 and IgG2) purified from ALL patients ($n = 4$) and normal control ($n = 4$) using DIG glycan differentiation kit (Fig. 5). The binding of GNA [specific for terminal Manα(1–3), (1–6) and (1–2)Man] to $IgG1_{ALL}$ and $IgG2_{ALL}$ was the weakest, being almost 38- ($P < 0.0001$) and 19-fold ($P < 0.0001$) lower than that of $IgG1_N$ and $IgG2_N$, indicating a lower content of terminal mannose residues in anti-9-*O*AcSGs$_{ALL}$, possibly resulting from masking of terminal mannose residues by Neu5Acs. Interestingly, binding with SNA [specific for Neu5-Acα(2–6)Gal/GalNAc] revealed a 5.9-fold higher binding to $IgG1_{ALL}$ than that of MAA (densitometric score being 73 257 ± 1749 versus 12 221 ± 937, respectively, $P < 0.0001$), reflecting the enhanced presence of Neu5Acs with a sub-terminal α2–6 linkage than α2–3 linkage. Similarly, $IgG2_{ALL}$ showed a 4.8-fold higher binding ($P < 0.001$) with SNA than MAA. On the contrary, both $IgG1_N$ and $IgG2_N$ demonstrated no difference in binding with SNA and MAA. An overall ~2-fold higher SNA binding was observed in both $IgG1_{ALL}$ and $IgG2_{ALL}$ ($P < 0.0001$) than in their normal counterparts.

The binding of DSA [specific for Galβ(1–4)GlcNAc] and PNA [specific for Galβ(1–3) GalNAc] with anti-9-*O*AcSGs was in general very low in both ALL patients and normal controls (Fig. 5).

Binding of ^{125}I-anti-9-*O*AcSGs with several Neu5Ac-binding lectins, e.g. WGA (GlcNAc/Neu5Ac), LPA (Neu5Ac), SNA and MAA, also indicated a higher degree of sialylation in IgG_{ALL} (Table 3). Other lectins, namely RCA, DBA, HPA, UEA and Achatinin-H, showed no marked difference in their binding. In contrast, a 5.9-fold higher ConA (α-Man, α-Glc) binding with IgG_N indicated an abundance of terminal mannose residues in normal antibodies.

Taken together, the observation suggests wide variations in glycosylation pattern specifically induced in 9-*O*AcSA-specific $IgG1_{ALL}$ and $IgG2_{ALL}$ as compared with their normal counterparts.

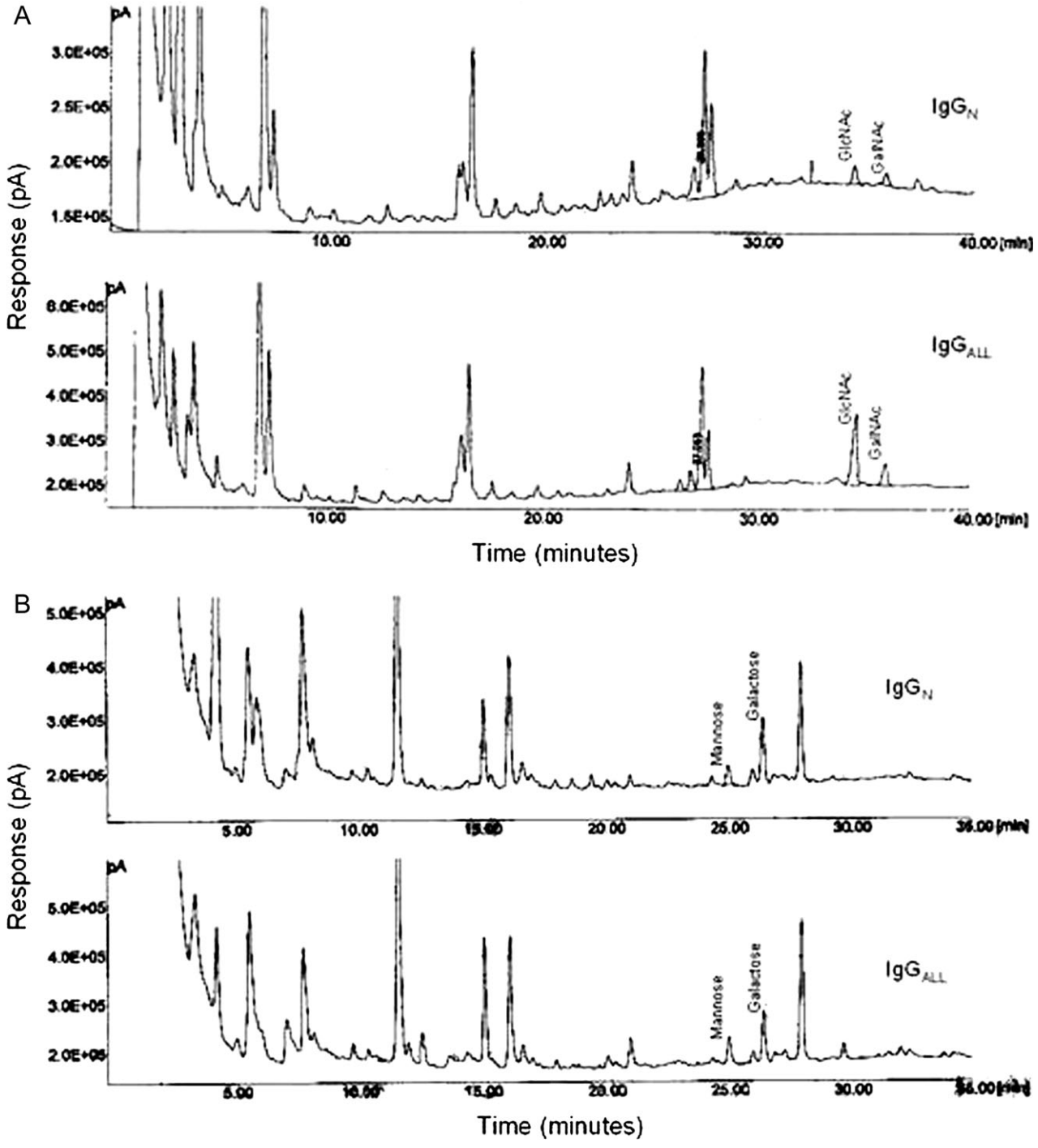

Fig. 4. Analysis of carbohydrate composition of anti-9-*O*AcSGs by GLC. The 9-*O*AcSA-specific IgG_{ALL} and IgG_N (100 μg each) were analyzed by GLC as stated in Methods. Response (in pA) was plotted against retention time (min). The representative profile of individual peaks revealed the differential expression of GlcNAc and GalNAc (A) and mannose and galactose (B).

9-OAcSA-specific IgG_{ALL} are less potent activators of U937 cells through Fcγ–FcγR interaction as compared with IgG_N

Following the blocking of Fab regions of purified anti-9-*O*AcSGs by BSM or purified 9-*O*AcSGs, the antibodies were incubated with IFNγ-sensitized U937 cells to compare their ability to activate these cells via interaction with FcγR. The generation of intracellular ROS was considered as an index for cell activation that was monitored using H_2DCFDA, which primarily detects H_2O_2 and hydroxyl radicals. Flow cytometric analyses revealed that anti-9-*O*AcSGs$_{ALL}$ caused a significantly lower level of FcγR activation as reflected from 45, 50

and 36% ROS-generating cells induced by total IgG, IgG1 and IgG2, respectively. In contrast, anti-9-*O*AcSGs$_N$ (total IgG and IgG1) demonstrated significantly higher ROS-generating cells (90 and 93%, respectively). Anti-9-*O*AcSGs$_N$ of IgG2 subclass, on the other hand, showed only 41% ROS-generating activity (Fig. 6A).

This observation was further validated using laser-scanning confocal microscopy wherein a decreased H_2DCFDA fluorescence was observed in cells that were targeted either with IgG or IgG1 of anti-9-*O*AcSGs$_{ALL}$, the FIU at 530 nm being 25.2 ± 3.7 and 30.8 ± 3.63, respectively (Fig. 6B and C). In contrast, cells probed with anti-9-*O*AcSGs$_N$ (IgG and IgG1) showed a 4.0- ($P < 0.0007$) and 4.5-fold ($P < 0.0003$) rise in ROS generation, the FIU at 530 nm being 100.0 ± 13.91 and 140.2 ± 16.30, respectively, in comparison to IgG and IgG1 of anti-9-*O*AcSGs$_{ALL}$. The IgG2 subclass anti-9-*O*AcSGs from both sources could not induce ROS generation and control sets showed negligible fluorescence.

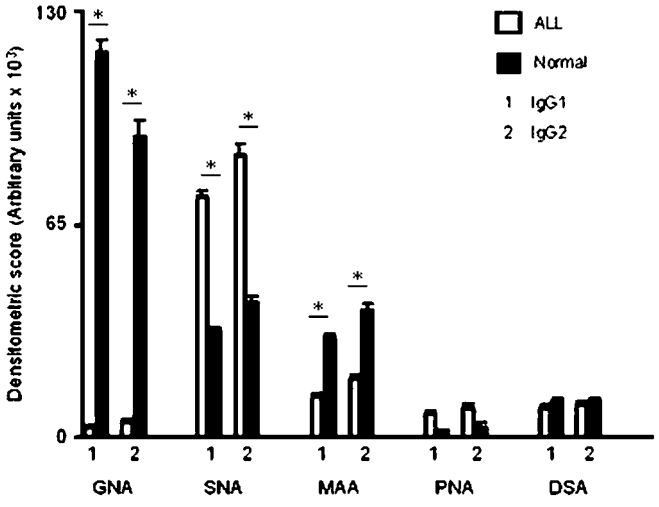

Fig. 5. Differential glycosylation pattern in anti-9-*O*AcSGs as detected by DIG enzyme assay. Purified 9-*O*AcSA-specific Igs (IgG1, $n = 4$, and IgG2, $n = 4$) from ALL patients (open bar) and normal individuals (filled bar) were analyzed for detection and linkage specificity of carbohydrate chains using different lectins, namely GNA, SNA, MAA, PNA and DSA, by DIG glycan differentiation kit as described in Methods. Results were reported as mean ± SD of densitometric score in arbitrary units from two independent experiments. Carboxypeptidase Y (GNA+), transferrin (SNA+), fetuin (SNA, MAA and DSA+) and asialofetuin (PNA and DSA+) were used as positive controls. *Significant differences between mean values, $P < 0.0001$.

Anti-9-OAcSGs from ALL patients (IgG$_{ALL}$) are poor activators of the classical complement pathway

The potential of anti-9-*O*AcSGs$_{ALL}$ (IgG1 and IgG2; 0.1, 0.5 and 1.0 μg) to activate the classical complement pathway was compared with anti-9-*O*AcSGs$_N$ using cell lines CEM-C7 (Fig. 7A) and REH (Fig. 7B) in the presence of 20% ALL sera and/or normal sera as the source of complement. Maximum differences in complement activation were observed with 1.0 lg concentration of anti-9-*O*AcSGs (complement activator).

IgG1$_N$ was found to be the only potent activator of classical complement pathway as reflected by a gradual increase in C3 deposition, maximum being 91–94% (Fig. 7A and B; Table 4). However, in both cell lines, 9-*O*AcSA-specific IgG1$_{ALL}$, IgG2$_{ALL}$ and IgG2$_N$ (0.1–1.0 μg) consistently showed low complement activation, C3 deposition being 21–29, 19–26 and 24–27%, respectively, using 1.0 μg of complement activators.

A similar amount of C3 deposition was observed irrespective of the source of complement used (ALL or normal human sera), suggesting undisturbed complement components in disease state.

To confirm that this C3 deposition was due to activation of the complement pathway, cells were incubated with antibodies or sera alone, or antibodies along with heat-inactivated sera. All controls consistently demonstrated an inability to trigger C3 deposition on both cell types, the range of C3 deposition being 2–16% (Table 4, Fig. 7A and B).

Table 3. Binding of ^{125}I-anti-9-*O*AcSGs with lectin beads

Lectin	Sugar and linkage specificity	Binding (%)			
		IgG1		IgG2	
		Patient	Normal	Patient	Normal
RCA	β-D-Gal	33.14	20.97	36.44	25.39
DBA	α-GalNAc	14.92	11.17	12.68	15.42
HPA	α- or β-D-GalNAc	17.58	12.33	19.53	13.41
UEA	α-L-Fuc	18.54	21.82	21.14	25.60
Con A	α-Man, α-Glc	7.79	46.25	12.14	50.76
WGA	GlcNAc/Neu5Ac	21.50	7.09	17.71	10.14
LPA	Neu5Ac	31.43	16.51	34.04	15.72
SNA	Neu5Acα2–6Gal/GalNAc	22.89	9.73	24.74	13.27
MAA	Neu5Acα2–3Gal	17.89	38.37	13.34	39.41
Achatinin-H	Neu5,9Ac$_2$α2–6β-D-GalNAc	17.05	14.72	15.33	20.13

Affinity-purified ^{125}I-anti-9-*O*AcSGs (IgG1 and IgG2, 0.2 μg) from patients and normal controls were incubated with Sepharose/agarose-bound lectins (20 μl) of different linkage and specificity as described in Methods. Unconjugated Sepharose/agarose beads served as controls. Binding (%) was determined from the specific binding of iodinated antibodies to lectin beads with respect to the total counts of the radio-labeled antibodies used for that particular set. All experiments were performed twice in triplicate, and a representative profile was reported here.

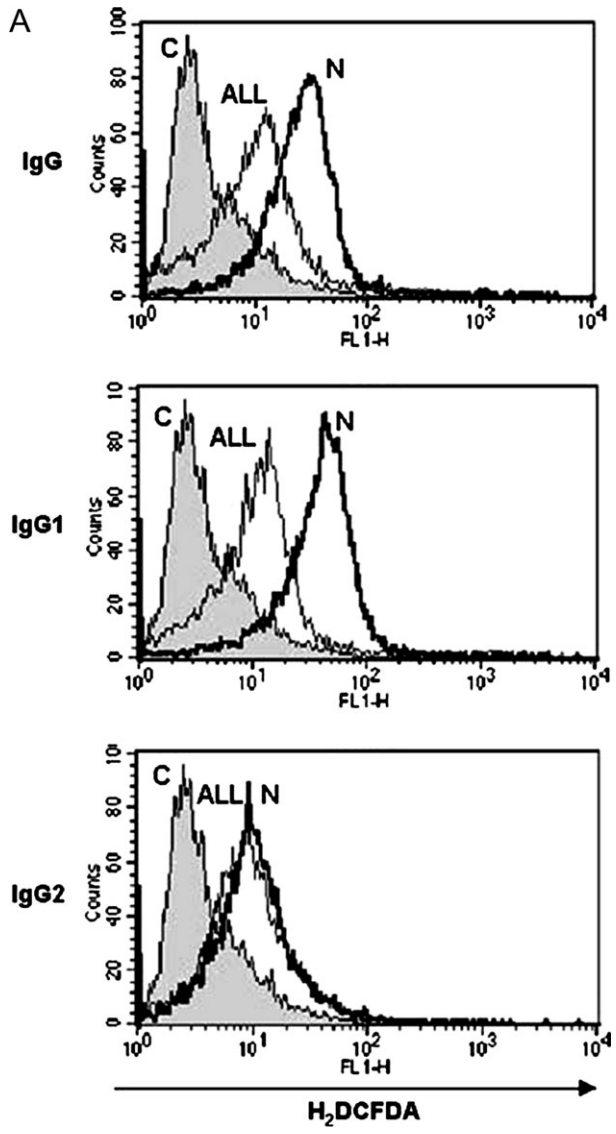

Fig. 6. Differential activation of FcγR by anti-9-*O*AcSGs as determined by intracellular respiratory burst. Fab-blocked anti-9-*O*AcSGs$_{ALL}$ and anti-9-*O*AcSGs$_N$ (IgG, IgG1 and IgG2) were compared for their FcγR-mediated U937 cell-activation potential as described in Methods. H_2DCFDA was used as the probe to monitor the generation of ROS by flow cytometry (A) and confocal microscopy (B). FACS analyses were represented by FL1-H histogram plot. Cells incubated with BSM and/or purified 9-*O*AcSGs served as controls (C, filled area). Anti-9-*O*AcSGs$_{ALL}$- and anti-9-*O*AcSGs$_N$-treated cells were shown as ALL and N, respectively (A). Confocal micrographs were reported as panels for fluorescence and phase contrast (B). (C) Bar graphs showing total ROS generation within U937 cells upon exposure to IgG, IgG1and IgG2 of anti-9-*O*AcSGs$_{ALL}$ (ALL) and anti-9-*O*AcSGs$_N$ (N). Data are represented in FIU at 530 nm. Significant differences between mean values: $*P < 0.0007$, $**P < 0.0003$.

Anti-9-OAcSGs$_{ALL}$ (IgG1 and IgG2) are weak mediators for cell-mediated cytotoxicity

To confirm differential functional potential of anti-9-*O*AcSGs, 9-*O*AcSA-specific IgG1 and IgG2 from ALL patients and normal individuals were used as mediators for cytotoxic activity of effector cells toward both T- and B-ALL cell lines. Optimum cytotoxicity was observed at 50 : 1 effector/target cell ratio. The 9-*O*AcSA-specific IgG1$_{ALL}$ and IgG2$_{ALL}$ were found to be poor mediators of antibody-dependent cell-mediated cytotoxicity (ADCC) as evidenced from 6–10% and 4–5% specific cell lyses in REH and CEM-C7 cell lines, respectively. Anti-9-*O*AcSGs$_N$ (IgG2) also showed a similar pattern of cytolysis (2–5%). In contrast to anti-9-*O*AcSGs$_N$ (IgG2), anti-9-*O*AcSGs$_N$ (IgG1) was capable of mediating a high degree of cytotoxicity in both the cell lines, mean specific cell lyses being 62% ($P < 0.0006$) and 42% ($P < 0.0007$) for REH and CEM-C7, respectively. Again, anti-9-*O*AcSGs$_N$ (IgG1) was found to be 6- ($P < 0.0009$) and 7-fold ($P < 0.001$) more effective in lysing REH and CEM-C7, respectively, than anti-9-*O*AcSGs$_{ALL}$ (IgG1).

Both IgG$_{ALL}$ and IgG$_N$ showed similar interactions with SpA and SpG

The interaction of ^{125}I-anti-9-*O*AcSGs (IgG1 and IgG2) purified from ALL patients and normal individuals with SpA and SpG was similar. The specific binding (counts per minute, mean ± SD) of IgG1$_{ALL}$ and IgG1$_N$ to SpA was 14 609 ± 673 versus 13 711 ± 541, and that to SpG was 17 021 ± 796 versus 17 935 ± 982, respectively. A similar pattern of binding was observed between IgG2$_{ALL}$ and IgG2$_N$ to SpA (11 323 ± 716 versus 13 010 ± 460) and SpG (14 709 ± 683 versus 12 907 ± 557).

Discussion

The conundrum of cancer immune surveillance indicates that the immune system not only can protect the host against tumor development but conversely also has the capacity to promote tumor growth, especially those with lower immunogenicity (18). Induction of disease-specific 9-*O*AcSGs on PBMC of childhood ALL (12, 33) was found to be highly immunogenic (15) and the diagnostic potential of anti-9-*O*AcSGs has been extensively demonstrated (16). However, assessment of their biological role in ALL is a relatively new domain in leukemia sialobiology. With this aim we were interested to explore the probable role of the disease-specific antibodies to provide an insight into the biology of this disease. The presence of a small fraction of antibodies against 9-*O*AcSGs mainly of IgG2 in normal human serum has long been identified (39), but progress in assigning it a biological role is still in its infancy.

The major findings of this investigation include the demonstration of (i) a shift in subclass distribution of anti-9-*O*AcSGs$_{ALL}$ toward IgG2 (Fig. 1), (ii) an alteration in total content and pattern of glycosylation including variation in the linkage-specific terminal Neu5Ac residues in anti-9-*O*AcSGs in ALL as compared with their normal counterparts (Figs 3–5) and (iii) defective triggering of a few Fc-glycosylation-sensitive effector functions in anti-9-*O*AcSGs$_{ALL}$ (Figs 6–8), while their antigen-binding property remained unaffected (Fig. 2).

A 3-fold higher amount of anti-9-*O*AcSGs in ALL patients' sera was present as compared with normal individuals. A defined specificity of different subclasses of purified anti-9-*O*AcSGs toward the glycotope Neu5,9Ac$_2$α2–6β-D-GalNAc was documented by HA and HA inhibition assays (Tables 1 and 2), flow cytometry (Fig. 2A) and confocal microscopy (Fig. 2B).

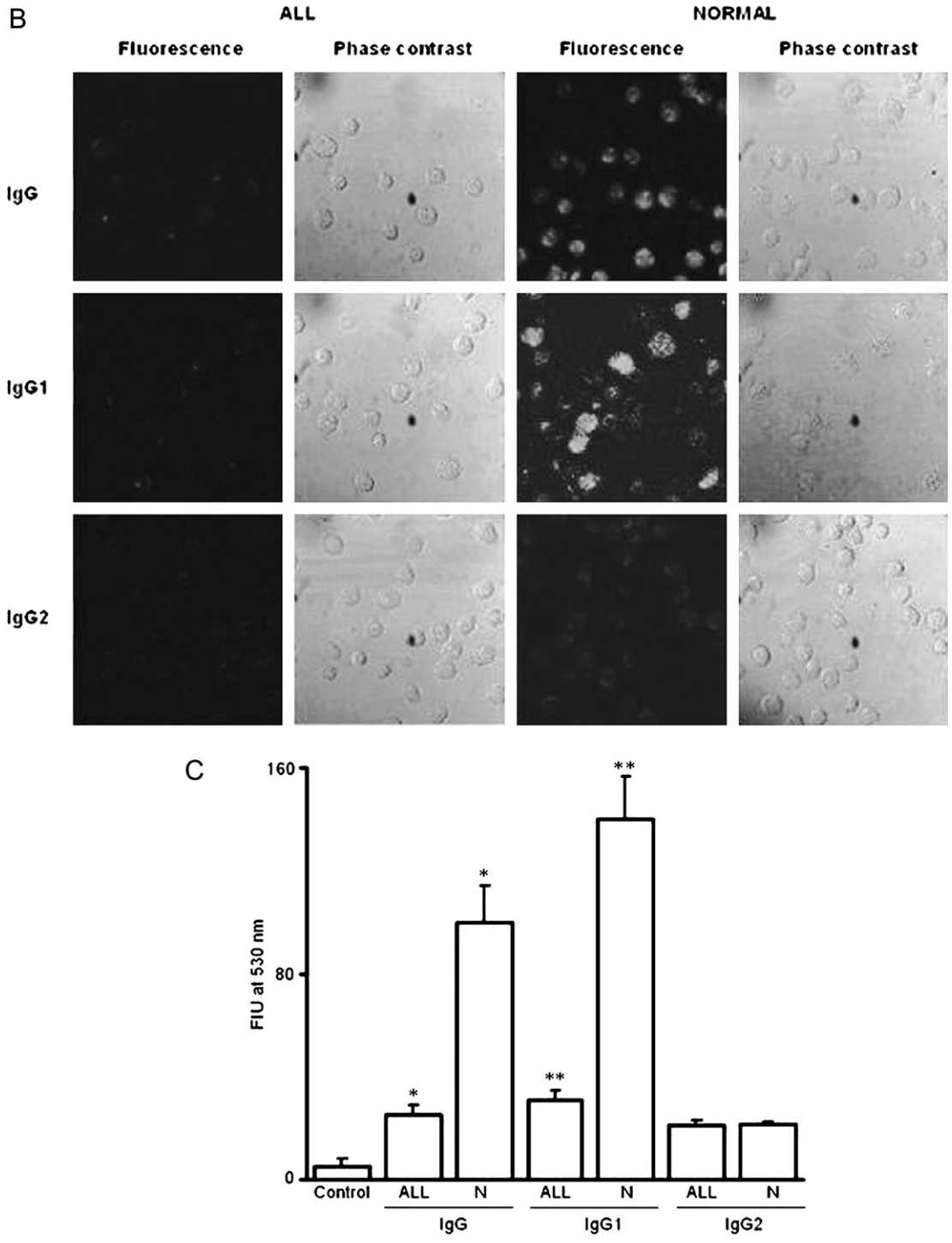

Fig. 6. *Continued.*

Both IgG1 and IgG2 of purified anti-9-*O*AcSGs$_{ALL}$ showed strong binding (87–99%) with PBMC$_{ALL}$, suggesting their fully functional antigen-binding capacity. The total absence of binding of anti-9-*O*AcSGs$_{ALL}$ with PBMC from various cross-reactive disorders like chronic myelogenous leukemia, acute myelogenous leukemia (AML), chronic lymphocytic leukemia (CLL), non-Hodgkin's lymphoma (NHL), adult ALL, aplastic anemia and thalassemia reiterated its disease specificity. Additionally, weak binding (8–14%) of anti-9-*O*AcSGs$_{ALL}$ (IgG1 and IgG2) with PBMC$_N$ reconfirmed a basal level of expression of 9-*O*AcSGs on PBMC$_N$ as indicated by our earlier observation (12).

Although differential distribution in levels of IgG subclasses is reported in several diseases, disease-specific distinct

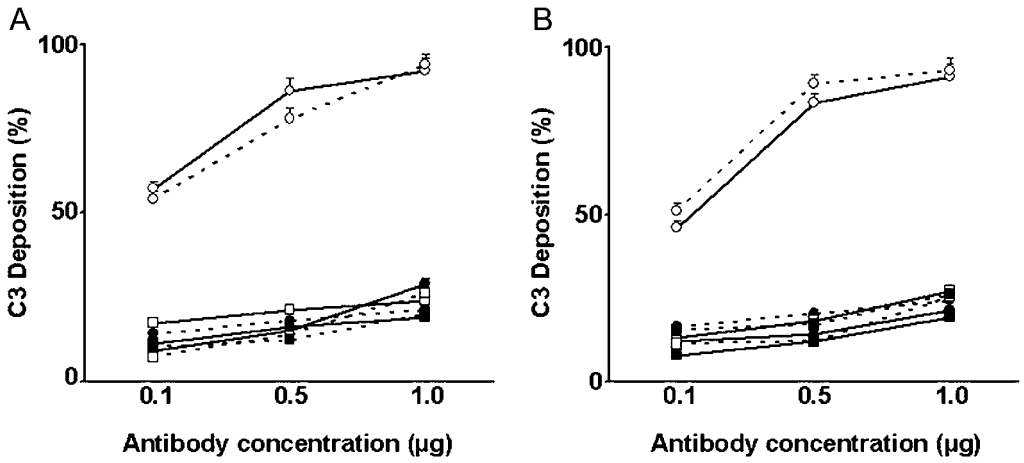

Fig. 7. Activation of the classical complement pathway by anti-9-*O*AcSGs$_{ALL}$ and anti-9-*O*AcSGs$_{N}$ (IgG1 and IgG2). CEM-C7 (T-ALL, A) and REH (B-ALL, B) cells (2×10^6) were incubated separately with anti-9-*O*AcSGs$_{ALL}$ and anti-9-*O*AcSGs$_{N}$ (0.1, 0.5 and 1.0 μg) at 37°C for 30 min (filled circle, ALL IgG1; open circle, normal IgG1; filled square, ALL IgG2; and open square, normal IgG2) using either 20% ALL sera (continuous lines) or normal sera (dotted lines) as the source of complement. Activation of classical complement pathway was monitored by C3 deposition on cell surface using ^{125}I-anti-C3 mAb as described in Methods. C3 deposition was represented as percentage of specific binding of antibody (mean ± SD of triplicate values). Cells incubated with complement alone, antibody alone and antibody along with heat-inactivated complements served as controls.

Table 4. Impairment in complement activation by anti-9-*O*AcSGs$_{ALL}$ as demonstrated by C3 deposition

Complement activators	Complement sources	Cell lines	
		T-ALL	B-ALL
Anti-9-*O*AcSGs (1.0 μg)	Serum (20%)	CEM-C7	REH
IgG1$_{ALL}$	AS	29	21
	NS	21	24
IgG1$_{N}$	AS	92	91
	NS	94	93
IgG2$_{ALL}$	AS	19	19
	NS	20	26
IgG2$_{N}$	AS	24	27
	NS	26	25
—	AS	4	3
—	NS	2	8
IgG1$_{ALL}$	—	7	5
IgG1$_{N}$	—	3	6
IgG2$_{ALL}$	—	8	3
IgG2$_{N}$	—	4	5
IgG1$_{ALL}$	HI-AS	9	2
	HI-NS	11	8
IgG1$_{N}$	HI-AS	6	16
	HI-NS	13	4
IgG2$_{ALL}$	HI-AS	8	9
	HI-NS	5	7
IgG2$_{N}$	HI-AS	14	11
	HI-NS	8	5

Comparative potential of anti-9-*O*AcSGs (IgG1 and IgG2; 1.0 μg), purified from ALL patients and normal individuals, to activate the classical complement pathway was assessed using CEM-C7 (T-ALL) and REH (B-ALL) cells and 20% ALL sera (AS) and/or normal sera (NS) as the source of complement as described in Methods. The C3 deposition on the cell surface was considered as the index for complement activation and was presented as specific binding (%) of ^{125}I-anti-C3 mAb (mean of triplicate values). Cells incubated with complement alone, antibody alone and antibody along with heat-inactivated complements (HI-AS and HI-NS) served as controls. '—' indicates absence of particular component.

pattern is restricted to only a few. Accordingly, we attempted to analyze the status of 9-*O*AcSA-specific IgG subclasses in ALL. A predominance of IgG2 among all four subclasses in these children was demonstrated as evidenced by a 2.78-fold higher amount of IgG2$_{ALL}$ as compared with IgG1$_{ALL}$ (158.1 ± 5.57 versus 56.67 ± 3.63 μg ml^{-1}, respectively, Fig. 1). Interestingly, the level of 9-*O*AcSA-specific IgG2 was much higher (3-fold) in ALL patients than normal controls (158.1 ± 5.57 versus 51.26 ± 4.80 μg ml^{-1}, respectively), indicating the high immunogenicity of 9-*O*AcSGs in disease state and their efficient modulation for disease-specific alteration in isotype subclass switching toward IgG2. Patients with gynecological malignancies (40) and squamous cell carcinomas of head and neck (41) exhibited a characteristic decrease in IgG1 and an increase in IgG2 levels, relative to total IgG.

IgG, a multifunctional glycoprotein, comprises two distinct functional domains, expressing an antigen-specific binding site (IgG-Fab), while the IgG-Fc is responsible for triggering effector mechanisms through its interaction with specific ligands, e.g. cellular receptors (FcγR) and the C1 component of complement (42). The IgG-Fc is a homodimer comprising inter-chain disulfide-bonded hinge regions, glycosylated C_H2 domains and non-covalently paired C_H3 domains (42). Glycosylation of IgG-Fc has been shown to be essential for efficient activation of FcγR and C1 component of complement (42). The oligosaccharide profiles of the IgG are significantly influenced by disease stress, nutrient depletion or acid pH, resulting in hypogalactosylation or the addition of high mannose forms or failure of glycosylation (42). IgGs isolated from sera of patients with multiple myeloma, CLL and AML showed altered levels of fucose, Gal and bisecting GlcNAc as compared with normal (43–45). Based on these observations, we endeavored to analyze the glycosylation profile of different subclasses of monospecific polyclonal anti-9-*O*AcSGs specifically induced in sera of patients with childhood ALL and compared them with normal individuals.

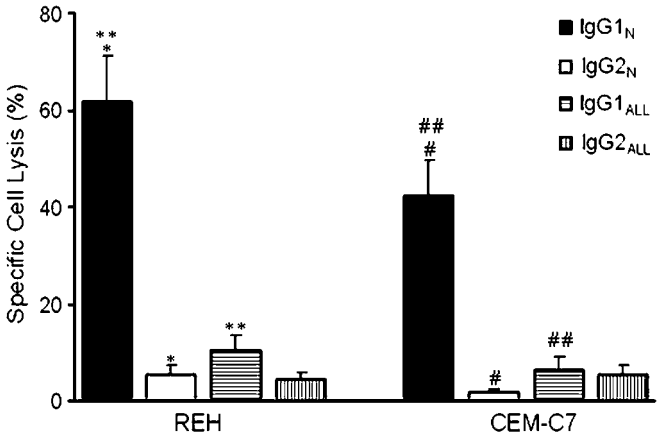

Fig. 8. Efficacy of anti-9-*O*AcSGs as potent mediator of cell-mediated cytotoxicity by ^{51}Cr-release assay. ALL cell lines (REH and CEM-C7) were labeled with $Na_2^{51}CrO_4$ in the presence and absence of purified antibodies (0.01 μg per 1×10^4 cells) and used as target cells. Four different types of antibodies [anti-9-*O*AcSGs$_N$ (IgG1, filled bar; IgG2, open bar) and anti-9-*O*AcSGs$_{ALL}$ (IgG1, ▤; IgG2, ▥)] were used as mediators of cytotoxicity. Freshly isolated normal human PBMC were used as effector cells. Target (1×10^4 cells per 100 μl per well) and effector cells were co-incubated and checked for released ^{51}Cr as described in Methods. Specific cell lyses (%) were calculated by normalizing the background cytotoxicity in the absence of added antibody. Optimum cytotoxicity (50 : 1 effector/target cell ratio) was demonstrated in bar graphs (mean ± SD of triplicate values). Significant differences between mean values: $*P < 0.0006$; $**P < 0.0009$; $\#P < 0.0007$; $\#\#P < 0.001$.

A wide variation in the degree of total glycosylation and specifically sialylation was observed in anti-9-*O*AcSGs as reflected by 2.1- and 3.6-fold higher level of glycosylation and sialylation in ALL patients as compared with their normal counterparts (Fig. 3A–C). This was confirmed by fluorimetric analysis that showed a similar increase in sialylation of IgG$_{ALL}$ as compared with IgG$_N$ (Fig. 3D). A significantly high proportion of SNA binding with IgG$_{ALL}$ (IgG1 and IgG2) as compared with MAA binding implies an enhanced induction of terminal Neu5Acα2–6Gal/GalNAc with concomitant reduction in terminal Neu5Acα2–3Gal (Fig. 5). IgG$_N$ showed a similar type of specificity toward SNA and MAA binding; however, the degree of binding was much lower than that of IgG$_{ALL}$. The conspicuously lower amount of terminal mannose both in IgG1$_{ALL}$ and IgG2$_{ALL}$, as reflected from GNA and Con A binding, could be attributed to their being masked by α2–6-linked Neu5Acs, possibly a characteristic feature of this disease (Fig. 5, Table 3).

Taken together, it has been convincingly demonstrated that 9-*O*AcSA-specific IgG$_{ALL}$ differ both in their content and nature of glycosylation as compared with IgG$_N$. Although a distinct disease-specific pattern of terminal and subterminal sugar moieties has emerged, a chemical analysis of total glycan structure of Igs from individual patients would be of utmost importance.

Glycoproteins are key components of the immune system effectors even though the attached sugar moieties often deviate greatly from their appropriate homogeneous geometrical array, thus affecting the activation of proper immune response. The ubiquity and diversity of protein glycosylation is not a paradox, but consistent with functional rules (46). Human IgG is predominantly glycosylated with N-linked carbohydrates and conserved glycosylation of the Fc region occurs at asparagine 297 (Asn^{297}), from which two opposing bi-antennary oligosaccharide chains protrude and interact. Crystallographic studies have shown that the two C$_H$2 domains do not interact by protein–protein contacts, but instead through oligosaccharides attached at the conserved site of Asn^{297} on each heavy chain. Protein–oligosaccharide and oligosaccharide–oligosaccharide interactions play a major role in maintaining the relative geometry of the C$_H$2 domains, consistent with the biological role of IgG (47).

As mediators of the humoral immune response, antibodies bind to specific antigens through Fab and then trigger biological responses by interacting through their Fc region with both cellular and soluble effector systems. It has been reported that heavy chain-linked conserved glycans of IgGs at Asn^{297} significantly contribute to their effector properties by influencing the complement activation via the classical pathway, which begins with the binding of C1q component of the complement to the C$_H$2 domain of the IgG molecule, binding of IgGs to FcγR and subsequent cellular function, induction of ADCC and also rapid elimination of the antigen–antibody complexes from the circulation (42, 48, 49).

Analysis of effector function of anti-9-*O*AcSGs revealed that FcγR-activating capacity was much lower in IgG1$_{ALL}$ as evidenced from a decrease in the percentage of ROS-generating cells, when U937 cells, known to contain a high amount of FcγRI on their surface, were targeted with Fab-blocked antibodies, suggesting their functional impairment (Fig. 6A). Whereas IgG1$_N$ was fully capable of activating 91% U937 cells for ROS generation. This was corroborated with confocal microscopy (Fig. 6B and C). Similarly, the capacity of FcγR triggering was decreased both in IgG2$_{ALL}$ and IgG2$_N$, ROS positivity being 35 and 39%, respectively (Fig. 6A). The efficiency of normal human IgG2 in binding to FcγR is reported to be the lowest among all the subclasses of IgG, the efficiency decreases in the following order IgG1 = IgG3 > IgG4 ⋙ IgG2 (49). The predominance of 2.8-fold increased production of 9-*O*AcSA-specific IgG2 (Fig. 1) along with low amounts of non-functional IgG1 in ALL patients suggests the inappropriate immune surveillance.

The impaired functioning of 9-*O*AcSA-specific IgG1$_{ALL}$ and IgG2$_{ALL}$ has further been demonstrated by their diminished complement activation as reflected from less C3 deposition (Fig. 7, Table 4). Notably, IgG1$_N$ was found to be the only potential activator of classical complement pathway. Considering the fact that antibody binding to C1q does not guarantee the activation of C1 (50), we checked the C3 deposition, a downstream component, to get the assurance of activated complement cascade. Nature of the terminal sugars on Fc-glycans is known to influence the activation of C1 (42).

ADCC experiments using IgG1 and IgG2 subclasses of anti-9-*O*AcSGs$_{ALL}$ and anti-9-*O*AcSGs$_N$ as mediators clearly demonstrate the inability of anti-9-*O*AcSGs$_{ALL}$ to elicit any specific cytolysis (Fig. 8), thereby further strengthening the observed impairment of their proper biological functioning as evidenced from their low FcγR-activating capacity (Fig. 6A–C) and diminished complement activation potential (Fig. 7, Table 4).

SpA and SpG are known to bind to IgG-Fc at the interface between the C$_H$2 and C$_H$3 domains of the Fc through

hydrophobic interactions (51). X-ray crystallographic and NMR studies clearly illustrated the negligible role of differences in IgG-Fc glycosylation in their SpA and SpG binding (42). Interestingly, our observation also demonstrates the similar binding profile of anti-9-*O*AcSGs (IgG1 and IgG2) with Protein A and G, irrespective of the source of antibodies, i.e. patient or normal sera.

In spite of several attempts by using glycosylation inhibitor, site-directed mutagenesis and enzymatic addition of particular sugar to analyze the direct influence of distinct glycosylation profile on functional activity of IgG, the underlying mechanism still remains unclear (49). However, dramatic differences in functional activity of IgGs were observed between fully glycosylated and molecular variants with selectively modified glycosylation or aglycosylated forms (42). If receptor/ligand interactions are modulated by glycosylation differences, the protective effector mechanisms activated by an oligoclonal-specific antibody population could be dependent on the predominant glycoforms present (49). This suggests an interesting possibility since IgG antibody responses can be subclass and clonally restricted and the glycosylation profiles of these antibodies may also be restricted as observed for IgG myeloma proteins (49). Surprizingly, passive immunization with anti-tumor antibodies did not protect against tumor growth, in many cases they actually enhanced the growth of the tumor (52).

In summary, this report established significant differences in glycosylation (mainly sialylation) and several functional properties between the 9-*O*AcSA-specific Igs from ALL patients and normal individuals and suggested anti-9-*O*AcSGs-mediated impairment of proper immune clearance in ALL. In the future, we hope to address the direct correlation between observed structural heterogeneity in glycosylation and the impaired functions of anti-9-*O*AcSGs in ALL by analyzing the conformational changes of Fc-carbohydrates, changes in topography of ligand-binding sites and subsequently their functional properties using different truncated glycoforms and also considering an individualistic approach. Studies with soluble recombinant FcγRI or FcγR knockouts would also provide confirmatory evidence.

Considering the phenomena of subclass switching from IgG1 to IgG2, their heterogeneous glycosylation, preferential sialylation along with the impairment of function (activation of FcγR and complement) in ALL patients, the generation of customized antibody constructs bearing functional Fc domain of anti-9-*O*AcSGs-IgG1, having a homogenous glycoform and a predetermined profile of functional potential, might lead to their effective functioning. Such customized antibodies might be used in conjugation with cytokine therapy to activate *in vivo* anti-cancer pathways for proper immune surveillance in pediatric ALL.

Acknowledgements

We extend our sincere thanks to Mr Ranjan Dutta of Bose Institute for his kind help in flow cytometry. We thank Alfredo Toreno, Servicio de Immunologia, Centro Nacional de Microbiologia, Instituto de Salud Carlos III, Majadahonda, Madrid, Spain, and R. Vlasak, CEO, Applied Biotechnology, GmbH, Austria, for their generous gift of anti-C3 antibody and *O*-acetyl esterase, respectively. We thank Mrs Sumi Bandyopadhyay for her kind help with ^{125}I-anti-C3 antibody. S.B. is a Senior Research Fellow of CSIR.

Abbreviations

ADCC	antibody-dependent cell-mediated cytotoxicity
ALL	acute lymphoblastic leukemia
AML	acute myelogenous leukemia
Asialo BSM	de-sialylated BSM
BSM	bovine submaxillary mucin
CLL	chronic lymphocytic leukemia
de-*O*Ac BSM	de-*O*-acetylated BSM
DBA	*Dolichos biflorus* agglutinin
DIG	digoxigenin
DSA	*Datura stramonium* agglutinin
FIU	fluorescence intensity unit
Gal	galactose
GalNAc	*N*-acetyl galactosamine
GLC	gas–liquid chromatography
GlcNAc	*N*-acetyl glucosamine
GNA	*Galanthus nivalis* agglutinin
HA	hemagglutination
H_2DCFDA	2′,7′-dichlorofluorescein diacetate
HPA	*Helix pomatia* agglutinin
LPA	*Limulus polyphemus* agglutinin
MAA	*Maackia amurensis* agglutinin
Neu5Ac	sialic acid
NHL	non-Hodgkin's lymphoma
9-*O*AcSa	9-*O*-acetylated sialic acid
9-*O*AcSGs	9-*O*-acetylated sialoglycoconjugates
PNA	peanut agglutinin
ROS	reactive oxygen species
SNA	*Sambucus nigra* agglutinin
SpA	Staphylococcal protein A
SpG	Streptococcal protein G
TBS	Tris-buffered saline
UEA	*Ulex europaeus* agglutinin
WGA	wheat germ agglutinin

References

1 Pui, C. H., Campana, D. and Evans, W. E. 2001. Childhood acute lymphoblastic leukemia—current status and future perspectives. *Lancet Oncol.* 2:597.
2 Bjorklund, E., Majur, J., Soderhall, S. and Porwit-MacDonald, A. 2003. Flow cytometric follow-up of minimal residual disease in bone marrow gives prognostic information in children with acute lymphoblastic leukemia. *Leukemia* 17:138.
3 Mandal, C., Chatterjee, M. and Sinha, D. 2000. Investigation of 9-*O*-acetylated sialoglycoconjugates in childhood acute lymphoblastic leukemia. *Br. J. Haematol.* 110:801.
4 Kelm, S. and Schauer, R. 1997. Sialic acids in molecular and cellular interactions. *Int. Rev. Cytol.* 175:137.
5 Klein, A. and Roussel, P. 1998. *O*-Acetylation of sialic acids. *Biochimie* 80:49.
6 Angata, T. and Varki, A. 2002. Chemical diversity in the sialic acids and related alpha-keto acids: an evolutionary perspective. *Chem. Rev.* 102:439.
7 Sinha, D., Chatterjee, M. and Mandal, C. 2000. *O*-Acetylated sialic acids—their detection, biological significance and alteration in diseases. *Trends Glycosci. Glycotechnol.* 12:17.
8 Sen, G. and Mandal, C. 1995. The specificity of the binding site of Achatinin$_H$, a sialic-acid binding lectin from *Achatina fulica*. *Carbohydr. Res.* 268:115.
9 Mandal, C. and Basu, S. 1987. A unique specificity of a sialic acid binding lectin Achatinin$_H$ from the hemolymph of *Achatina fulica* snail. *Biochem. Biophys. Res. Commun.* 148:795.
10 Basu, S., Mandal, C. and Allen, A. K. 1988. Chemical-modification studies of a unique sialic acid binding lectin from the snail *Achatina fulica*. *Biochem. J.* 254:195.
11 Mandal, C., Basu, S. and Mandal, C. 1989. Physicochemical studies on AchatininH, a novel sialic acid binding lectin. *Biochem. J.* 257:65.
12 Sinha, D., Mandal, C. and Bhattacharya, D. K. 1999. Identification of 9-*O* acetyl sialoglycoconjugates (9-*O*AcSGs) as biomarkers in

childhood acute lymphoblastic leukemia using a lectin, Achatinin$_H$, as a probe. *Leukemia* 13:119.
13 Pal, S., Ghosh, S., Mandal, C. *et al.* 2004. Purification and characterization of 9-*O*-acetylated sialoglycoproteins from leukemic cells and their potential as immunological tool for monitoring childhood acute lymphoblastic leukemia. *Glycobiology* 14:859.
14 Pal, S., Chatterjee, M., Bhattacharya, D. K., Bandhyopadhyay, S., Mandal, C. and Mandal, C. 2001. *O*-acetyl sialic acid specific IgM as a diagnostic marker in childhood acute lymphoblastic leukemia. *Glycoconj. J.* 18:529.
15 Pal, S., Chatterjee, M., Bhattacharya, D. K., Bandhyopadhyay, S. and Mandal, C. 2000. Identification and purification of cytolytic antibodies directed against *O*-acetylated sialic acid in childhood acute lymphoblastic leukemia. *Glycobiology* 10:539.
16 Pal, S., Bandyopadhyay, S., Chatterjee, M. *et al.* 2004. Antibodies against 9-*O*-acetylated sialoglycans: a potent marker to monitor clinical status in childhood acute lymphoblastic leukemia. *Clin. Biochem.* 37:395.
17 Bandyopadhyay, S., Mukherjee, K., Chatterjee, M., Bhattacharya, D. K. and Mandal, C. 2004. Detection of immune-complexed 9-*O*-acetylated sialoglycoconjugates in the sera of patients with pediatric acute lymphoblastic leukemia (ALL). *J. Immunol. Methods.* in press.
18 Dunn, G. P., Bruce, A. T., Ikeda, H., Old, L. J. and Schreiber, R. D. 2002. Cancer immunoediting: from immunosurveillance to tumor escape. *Nat. Immunol.* 3:991.
19 Khong, H. T. and Restifo, N. P. 2002. Natural selection of tumor variants in the generation of "tumor escape" phenotypes. *Nat. Immunol.* 3:999.
20 Takeda, K., Smyth, M. J., Cretney, E. *et al.* 2002. Critical role for tumor necrosis factor-related apoptosis-inducing ligand in immune surveillance against tumor development. *J. Exp. Med.* 195:161.
21 Catlett-Falcone, R., Landowski, T. H., Oshiro, M. M. *et al.* 1999. Constitutive activation of stat3 signaling confers resistance to apoptosis in human U266 myeloma cells. *Immunity* 10:105.
22 Marincola, F. M., Jaffee, E. M., Hicklin, D. J. and Ferrone, S. 2000. Escape of human solid tumors from T-cell recognition: molecular mechanisms and functional significance. *Adv. Immunol.* 74:181.
23 Kaplan, D. H., Shankaran, V., Dighe, A. S. *et al.* 1998. Demonstration of an interferon γ–dependent tumor surveillance system in immunocompetent mice. *Proc. Natl Acad. Sci. USA* 95:7556.
24 Burns, C. P., Armitage, J. O., Frey, A. L., Dick, F. R., Jordan, J. E. and Woolson, R. F. 1981. Analysis of the presenting features of adult acute leukemias: the French-American-British classification. *Cancer* 47:2460.
25 Murphy, W. H. and Gottschalk, A. 1961. Studies on mucoproteins, VII. The linkage of the prosthetic group to aspartic and glutamic acid residues in bovine submaxillary gland mucoprotein. *Biochim. Biophys. Acta* 52:349.
26 Lowry, O. H., Rosebrough, N. J., Farr, A. L. and Randall, R. J. 1951. Protein measurement with folin phenol reagent. *J. Biol. Chem.* 193:265.
27 Chatterjee, M., Chava, A. K., Kohla, G. *et al.* 2003. Identification and characterization of adsorbed serum sialoglycans on *Leishmania donovani* promastigotes. *Glycobiology* 13:351.
28 Shukla, A. K. and Schauer, R. 1982. Fluorimetric determination of unsubstituted and 9(8)-*O*-acetylated sialic acids in erythrocyte membranes. *Hoppe-Seyler's Z. Physiol. Chem.* 363:255.
29 Kohn, J. and Wilchek, M. 1982. A new approach (cyano-transfer) for cyanogen bromide activation of sepharose at neutral pH, which yields activated resin, free of interfering nitrogen derivatives. *Biochem. Biophys. Res. Commun.* 107:878.
30 Reuter, G., Pfeil, R., Stoll S. *et al.* 1983. Identification of new sialic acids derived from glycoprotein of bovine submandibular gland. *Eur. J. Biochem.* 134:139.
31 Laemmli, U. K. and Favre, M. 1970. Cleavage of structural proteins during the assembly of the head of bacteriophage T4. *Nature* 227:680.
32 Coligan, E. J., Kruisbeek, M. A., Margulies, H. D., Shevach, M. E. and Strober, W. 1993. Labeling antibody with fluorescein isothiocyanate (FITC). In Coligan, E. J., Kruisbeek, M. A., Margulies, H. D., Shevach, M. E. and Strober, W., eds, *Current Protocols in Immunology. National Institutes of Health*, vol. 1, p. 5.3.2. John Wiley & Sons, New York, USA.
33 Pal, S., Ghosh, S., Bandyopadhyay, S. *et al.* 2004. Differential expression of 9-*O*-acetylated sialoglycoconjugates on leukemic blasts: a potential tool for long-term monitoring of children with acute lymphoblastic leukemia. *Int. J. Cancer*, 111:270.
34 Sloneker, J. H. 1972. Gas–liquid chromatography of alditol acetates. In Whistler, R. L. and BeMiller, J. N., eds, *Methods in Carbohydrate Chemistry, VI*, p. 20. Academic Press Inc., New York.
35 Hunter, W. M. 1978. In Weir, D. M., ed., *Handbook of Experimental Medicine*, p. 14.1. Blackwell Scientific, London.
36 Dominguez, M., Moreno, I., Lopez-Trascasa, M. and Torano, A. 2002. Complement interaction with trypanosomatid promastigotes in normal human serum. *J. Exp. Med.* 195:451.
37 Coligan, E. J., Kruisbeek, M. A., Margulies, H. D., Shevach, M. E. and Strober, W. 1993. 51Cr release assay of antibody-dependent cell-mediated cytotoxicity (ADCC) In Coligan, E. J., Kruisbeek, M. A., Margulies, H. D., Shevach, M. E. and Strober, W., eds, *Current Protocols in Immunology. National Institutes of Health*, vol. 1, p. 7.27.1. John Wiley & Sons, New York, USA.
38 Schauer, R. 2004. Sialic acids: fascinating sugars in higher animals and man. *Zoology* 107:49.
39 Siebert, H. C., Von der Lieth, C. W., Dong, X. *et al.* 1996. Molecular dynamics-derived conformation and intramolecular interaction analysis of the *N*-acetyl-9-*O*-acetylneuraminic acid-containing ganglioside$_{GD1a}$ and NMR-based analysis of its binding to a human polyclonal immunoglobulin G fraction with selectivity for *O*-acetylated sialic acids. *Glycobiology* 6:561.
40 Felsner, P., Steinschifter, W., Fischer, M. *et al.* 2000. The tumor-associated shift in immunoglobulin G1/G2 is expressed at the messenger RNA level of peripheral B lymphocytes in patients with gynecologic malignancies. *Cancer* 88:461.
41 Anderhuber, W., Steinschifter, W., Schauenstein, E. *et al.* 1999. The IgG1/IgG2 subclass shift—a sensitive, tissue non-specific marker for malignancy. Diagnostic performance with squamous cell carcinoma of the head and neck. *Br. J. Cancer* 79:1777.
42 Jefferis, R., Lund, J. and Pound, J. D. 1998. IgG-Fc-mediated effector functions: molecular definition of interaction sites for effector ligands and the role of glycosylation. *Immunol. Rev.* 163:59, and references therein.
43 Jefferis, R., Lund, J., Mizutani, H. *et al.* 1990. A comparative study of the N-linked oligosaccharide structures of human IgG subclass proteins. *Biochem. J.* 268:529.
44 Farooq, M., Takahashi, N., Arrol, H., Drayson, M. and Jefferis, R. 1997. Glycosylation of polyclonal and paraprotein IgG in multiple myeloma. *Glycoconj. J.* 14:489.
45 Kondo, A., Hosokawa, Y., Kiso, M., Hasegawa, A. and Kato, I. 1994. Analysis of oligosaccharides of human IgG from serum of leukemia patients. *Biochem. Mol. Biol. Int.* 32:897.
46 Rudd, P. M., Elliott, T., Cresswell, P., Wilson, I. A. and Dwek, R. A. 2001. Glycosylation and the immune system. *Science* 291:2370.
47 Deisenhofer, J. 1981. Crystallographic refinement and atomic models of a human Fc fragment and its complex with fragment B of protein A from *Staphylococcus aureus* at 2.9-and 2.8-A resolution. *Biochemistry* 20:2361.
48 Krotkiewski, H. 1999. Carbohydrate moiety of immunoglobulins in health and pathology. *Acta Biochim. Pol.* 46:341.
49 Jefferis, R. and Lund, J. 2002. Interaction sites on human IgG-Fc for FcγR: current models. *Immunol. Lett.* 82:57, and references therein.
50 Duncan, A. R. and Winter, G. 1988. The binding site for C1q on IgG. *Nature* 332:738.
51 Burton, D. R. 1985. Immunoglobulin G—functional sites. *Mol. Immunol.* 22:161.
52 Goldsby, R. A., Kindt, T. J., Osborne, B. A., eds. 2000. *Kuby Immunology*, 4th edn, p. 551. W. H. Freeman and Company, New York.